AL-QADISIYAH JOURNAL FOR ENGINEERING SCIENCES 12 (2019) 135–143

Contents lists available at http://qu.edu.iq

Al-Qadisiyah Journal for Engineering Sciences

Journal homepage: http://qu.edu.iq/journaleng/index.php/JQES

Pellet Softening Process for the Removal of the Groundwater Hardness; Modelling and Experimentation

Fatin A. Ashoor [a]*, Amer D. Zmat [a] and Muthanna H. AlDahhan [b]

[a] *Department of Chemical engineering, University of Al-Qadisiyah, Al-Qadisiyah, Iraq.*

[b] *Multiphase Reactors and Applications Laboratory mReal, Department of Chemical and Biochemical Engineering, Missouri University of Science and Technology, Rolla, MO 65409-1230, USA*

ARTICLE INFO

Article history:
Received 24 July 2019
Received in revised form 04 September 2019
Accepted 12 September 2019

Keywords:
Pellet reactor
Groundwater softening
water hardness removal
Crystillization

ABSTRACT

A lab scale pellet reactor (PR) was designed and fabricated to carry out extensive investigations on the removal efficiency of the hardness of groundwater. The groundwater of 2200 – 2600 mg/L hardness was collected from Abdulla Ibnalhassan wells area located at the west desert of Al-Shinafiyah district (70 km to the southwest of Al-Dewaniyah city, Iraq). Both hydrodynamic parameters of the pellet reactor (porosity and fluidized bed height) and the parameters of calcium carbonate crystallization process (calcium carbonate equilibrium, pellet size, and density) were modeled and compared with the experimental results of the lab scale pellet reactor. The comparison showed that fair agreement between modeled and measured results was observed. The removal efficiency of both calcium and magnesium ions were 62.5-99% and 83-99% respectively. The removal efficiency was found to be strongly dependent on pH and the ratio of NaOH solution flow rate to the groundwater flow rate in the pellet reactor.

1. Introduction

Pellet Reactor (PR) is increasingly used to remove the hardness of groundwater. PR is favored over other softening processes of groundwater due to its low produced sludge, low capital cost, and low maintenance. The main reactions of groundwater softening are shown below [1];

$$2NaOH + Ca^{+2} + H_2CO_3 \rightarrow CaCO_3 + 2Na^{+} + 2H_2O$$

$$NaOH + Ca^{+2} + HCO_3^{-} \rightarrow Na^{+} + CaCO_3 + H_2O$$

PR is simply a cylindrical column filled to a certain depth with a seeding material (sand particles) to crystalize Ca+2 ions and form calcium carbonate on its surface [2]. The literature presents many research articles that cover most important aspects of groundwater softening process and PR role [3]. The reactor is firstly filled with granular materials such as sand and quartz. The hard water and softening agent are pumped to the reactor at suitable flow rates to fluidize sand granules and stimulate crystallization of $CaCO_3$ [4]. Crystallization of $CaCO_3$ on the surfaces of sand particles, in a pellet reactor, can be divided into two stages: nucleation and growth up [5]. Nucleation may be described as $CaCO_3$ crystals formation. Growth up is the process in which $CaCO_3$ crystals crystallize at the surface of sand or quartz granules in the form of layers [6]. Mahvi et al. [7] successfully modeled the hydrodynamics and growth rate of crystals of a softening lab scale fluidized bed reactor. He used two-step crystal growth model rather

* *Corresponding author.* Tel.: +964(0)781706291.
E-mail address: fatinashoor80@gmail.com (Fatin A. Ashoor)

https://doi.org/10.30772/qjes.v12i3.603
2411-7773/© 2019 University of Al-Qadisiyah. All rights reserved.

Nomenclature

dg	Average diameter of sand grain (m)
dg1	Average diameter of sand grain , type 1 (m)
dg2	Average diameter of sand grain , type 2 (m)
dp	Average diameter of calcite Pellet (m)
dp1	Average diameter of calcite Pellet ,type 1 (m)
dp2	Average diameter of calcite Pellet ,type 2 (m)
Reh	Hydraulic Reynolds number
Sc	Schmidt number
Sh	Sherwood number
SI	Saturation Index
IS	Ionic strength (mmol/L)
Fw	Flow of water (L/s)
Fn	Flow of NaOH solution (L/s)
G	Gravitational acceleration (m/s^2)
K	Crystallization kinetics ($L\ m\ s^{-1}\ mmol^{-1}$)
Ks	Solubility product ($mmol^2/L^2$)
kT	Reaction rate ($L\ m\ s^{-1}\ mmol^{-1}$)
kT20	Reaction rate at 20◦C ($L\ m\ s^{-1}\ mmol^{-1}$)
kf	Transport rate of supersaturated water to the pellet surface ($L\ m\ s^{-1}\ mmol^{-1}$)
Δxo	Fixed Bed height m
Δx	Fluidized Bed height (m)
P	Bed porosity
po	Fixed Bed porosity
mc	Total mass of attached $CaCO_3$ (Kg)
mc1	Mass of attached $CaCO_3$ of the first sand type (Kg)
Mc	Mass of attached $CaCO_3$ of the second sand type (Kg)
y1	Volume fraction of sand grain , type 1
y2	Volume fraction of sand grain , type 2
Mc	$CaCO_3$ molecular weight (g/mmol)
Ac	Cross section area of reactor (m^2)
N	Number of grains
T	Water temperature (ºC)
$[Ca^{+2}]o$	Initial calcium concentration of groundwater (mmol/ L)
$[Ca^{+2}]m$	Modeled calcium concentration of treated groundwater (mmol/ L)
$[Ca^{+2}]e$	Measured calcium concentration of treated groundwater (mmol/ L)
t	Time (s)
Df	Diffusion coeffient of groundwater (m^2/s)
S	Specific surface area of calcite pellets (m^2/m^3)
C	Crystallization rate ($mmol\ L^{-1}\ s^{-1}$)

Greek symbols

Θ	Valency of ion
v	Kinematic viscosity of groundwater (m^2/s)
ρg	Density of seeding material (kg/m^3)
ρc	Density of $CaCO_3$ (kg/m^3)
ρp	Average density of calcite pellets (kg/m^3)
ρ_{p1}	Density of the first type of calcite pellets (kg/m^3)
ρ_{p2}	Density of the second type of calcite (kg/m^3)
ρw	Density of groundwater (kg/m^3)

than the over-all model. However, utilizing the two-step growth model suffers the lack of the surface-reaction order, and a lean fluidized bed reactor was proposed to include the surface-reaction order. The crystal growth process of low soluble salts seems more complicated than that of soluble salts. Then, a comparison between crystal growth kinetics of low soluble salts and the lean fluidized -bed crystallizers was demonstrated. As a consequence, the two-step growth model was found to be convenient for the assessment of crystal growth rates in the design of a liquid fluidized bed reactor [8]. Schagen, et al. [9] successfully simulated the pellet reactor and showed the effect of operational parameters (particle size and height of fluidized bed) on the removal efficiencies of the total hardness, calcium ions, and magnesium ions. They observed that maintaining the particle size, the reflux ratio, and the flow rates at optimum values can improve the pellet reactor performance. Schagen, et al. [10] **(**explained through a mathematical model the relationship between the size of the discharged pellets and the saturation rate of $CaCO_3$ in the treated water. They found that using smaller particle size of seeding materials led to a significant decrease in the saturation rate of $CaCO_3$ in treated water and improved the pellet reactor performance. Schagen, et al. [11] observed that the growth process of crystals of weakly soluble salts looks more intricate than that of high soluble salts. As a result, the two-step growth model was found to be suitable to simulate the rate of crystal growth in fluidized -bed reactor. Hu, et al. [12] developed a new mathematical model to study the effect of superficial velocity, particle size, and supersaturation on the rate of pellet particle growth and the fixed bed height growth rate. The study showed a linear relationship between the rate of particle growth and both superficial velocity and supersaturation.

The present research aims to study the removal efficiency of total hardness and the modeling of the pellet reactor which is composed of two parts; the first part includes the fluidization and fluidized bed hydrodynamics, while the second part is related to the crystallization process of $CaCO_3$ on the surfaces of seeding sand particles. The first part aims to model the relation between porosity, pellet diameter, and water velocity. The second part aims to model the crystallization of $CaCO_3$ as a shift in the equilibrium between the soluble and solid states of calcium.

2. Materials and Experimental Procedure

2.1. Materials

2.1.1. Groundwater

800 liters of groundwater were collected from Well(5) (area of study shown in Figure (1)) located in Abdulla Ibnalhassan area – Ash Shinafiyah district which is located 70 km to the south-west of Ad Diwaniyah city, Iraq. The depth of Well is 75 m. Calcium ion concentration, pH and electrical conductivity of groundwater are shown in Table (1).

Table 1. Groundwater Characteristics

parameter	value	Method	Model
PH	7-10.3	pH meter	SD300PH
E.C (µs/cm)	5380	EC meter	COND7110
Ca+2 (mg/L)	496- 664	titration	----------

2.1.2. Seeding Materials

Sand with a particle size of 0.426 - 2 mm was used as a seeding material to crystalize $CaCO_3$ on its surfaces. The density of the sand was 1.431 g/cm^3. Sand weight was measured before and after each experiment to determine the crystalized $CaCO_3$ on the surfaces of sand particles.

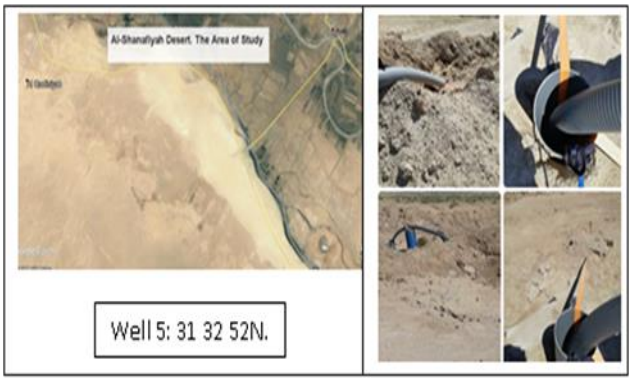

Figure 1: The Area of Study well 5 locations

Figure 2: Photo of the PR setup

2.1.3. NaOH Granules

NaOH granules from Sigma-Aldrich were used to prepare 0.625 molarity (2.5% mass concentration) NaOH solution. The characteristics of NaOH granules are shown in Table (2).

Table 2, The characteristics of NaOH granules

Density	2.13 g/cm^3
Molecular weight	40 gm/mole
Melting point	318 °C (604 °F; 591 K)
Boiling point	1,388 °C (2,530 °F; 1,661 K)

2.2. Experimental Procedure

2.2.1. Description of the Lab scale Pellet Reactor (PR)

The Lab scale PR shown in Figures (2, 3) was used for removing total hardness, calcium ions, and magnesium ions for groundwater. It is simply a fluidized bed column made from Plexiglas with an inner diameter of 6 cm and 170 cm height. The groundwater was fed (injected) through three nozzles mounted at the bottom plate of the column, while the NaOH solution was fed (injected) through one nozzle located at the center of the bottom plate. Nozzles details are schematically shown in Figure (4). The PR was equipped with two rotameters to measure both groundwater and NaOH solution flowrates. Water rotameter measuring range is (25-250) L/hr and NaOH solution rotameter are in the range of (6-30) L/hr. A sand filter with 12 cm outer diameter and 27 cm height was installed at the outlet of the PR to capture suspended materials. Two pressure measuring devices (0.0 – 6.0 bars) were installed on the lines of groundwater and NaOH solution supply for measuring pressure head of both supply lines. Three plastic tanks were used for storing groundwater, NaOH solution and treated water. 1.575 kg of a seeding material was used to fill a height of 42 cm of the FBR. The seeding material (sand) was brought from local sources.

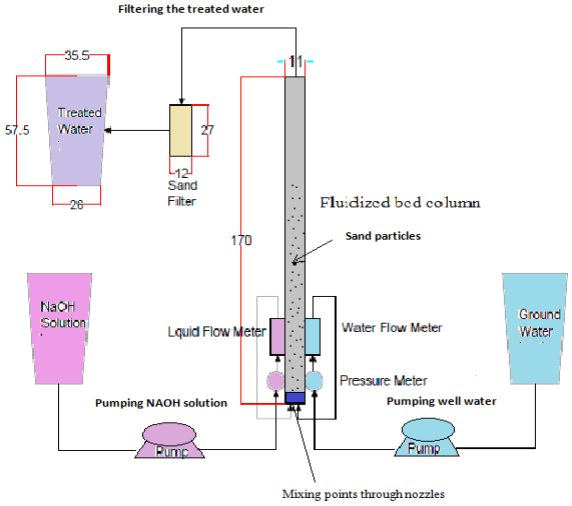

Figure 3: Schematic representation of water softening in PR

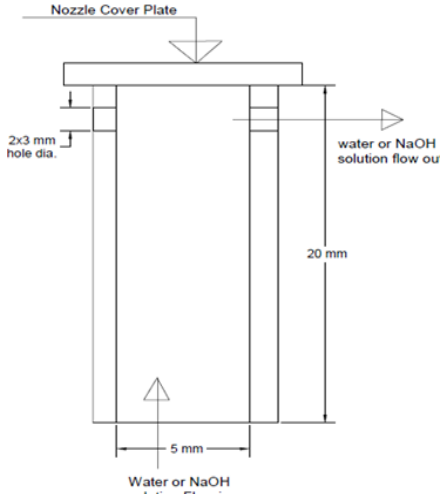

Figure 4: Schematic structure of the nozzle

3. Hydrodynamics of the PR (Ergun Model)

3.1. Porosity

Ergun model is widely utilized to calculate the porosity of the fluidized bed. Porosity is fundamentally calculated depending on balancing the pressure gradient across the fluidized bed, the mass of the pellets, and the acting drag force of the water on the calcite pellets[13].
The pressure gradient is expressed as:

$$\frac{\Delta p}{\Delta L} = (\rho_P - \rho_W).(1-P).g \quad (1)$$

The pressure gradient caused by the acting drag force of the water on the calcite pellets is represented by equation (2).

$$\frac{\Delta P}{\Delta L} = \frac{3}{2} C_{w1} \frac{v^2}{2} \frac{(1-p)}{p^3} \frac{\rho_w}{d_p} \quad (2)$$

C_{w1} is the drag coefficient which is expressed in terms of the hydraulic Reynolds Number (Re_h).

$$C_{w1} = 2.3 + \frac{150}{Re_h} \quad (3)$$

Where, $Re_h$is the particle Reynolds number, expressed using the following empirical equation [14]:

$$Re_h = \frac{2}{3} \frac{v\, d_p}{(1-p)\nu} \quad (4)$$

For the range of Re_h between (5 -100), C_{W1} is expressed in equation (5).

$$C_{w1} \approx \frac{125}{Re_h^{0.8}} \quad (5)$$

Finally, the general form of the porosity equation is:

$$\frac{p^3}{(1-p)^{0.8}} = 130 \frac{v^{1.2}}{g} \frac{\nu^{0.8}}{d_p^{1.8}} \frac{\rho_w}{\rho_{p-\rho_w}} \quad (6)$$

This equation has generally been utilized in most researches to find the porosity of the pellet softening column [14-16]**.**

3.1.1. The height of fluidized bed

The height of the fluidized zone of sand particle in the Pellet reactor is calculated as shown in equation (7) [17]:

$$\Delta x = (\frac{m_c}{\rho_c} + \frac{m_g}{\rho_g})(1-p)^{-1} As^{-1} \quad (7)$$

3.2. Crystallization of CaCO3 Modelling

3.2.1. 3 Pellet Size and Density

The pellet diameter relies on the accumulated mass of calcite ($CaCO_3$) on the surface of sand particles. The pellet size is determined using the following equation [17]:

$$dp = dg \sqrt[3]{1 + \frac{\rho_g}{\rho_c}\frac{m_c}{m_g}} \quad (8)$$

The calcite pellets density is represented by the mass of calcite ($CaCO_3$) on sand surface (m_c) and the mass of the sand particle (m_g), as follows [17]:

$$\rho_p = (m_c + m_g)(\frac{m_c}{\rho_c} + \frac{m_g}{\rho_g})^{-1} \quad (9)$$

Two types of sand have been used, so the pellet size and density of the two types are:

A- For $d_{g1} = 2\times10^{-3}$ m

$$m_{c\,1} = m_c \times y_1 \quad (10)$$

$$y_1 = \frac{(mg_1/\rho g_1)}{(mg/\rho g)} \quad (11)$$

B- For $d_{g2} = 0.5\times10^{-3}$ m

$$m_{c\,2} = m_c \times y_2 \quad (12)$$

$$y_2 = \frac{(mg_2/\rho g_2)}{(mg/\rho g)} \quad (13)$$

The average pellet size and density is calculated as follow:

$$\rho_p = 0.29 \times \rho_{p1\ at\ 2mm} + 0.71 \times \rho_{p2\ at\ 0.5\ mm} \quad (14)$$

$$d_p = 0.29 \times d_{p1\ at\ 2mm} + 0.71 \times d_{p2\ at\ 0.5\ mm} \quad (15)$$

3.2.2. The equilibrium of calcium carbonates ($CaCO_3$)

Calcium carbonate crystallization occurs when the solid and soluble calcium carbonate ($CaCO_3$) are in equilibrium [18].

$$Ca^{+2} + CO_3^{-2} \xleftrightarrow{ks} CaCO_3 \quad (16)$$

The activity coefficient (f) relies on the water ionic strength (IS) and it's represented by the following equation:

$$Log\,(f) = \Theta^2 . \frac{-0.5\sqrt{IS}}{\sqrt{1000} + \sqrt{IS}} = -0.0002\,IS \quad (17)$$

The ionic power determines the ionic strength of solutions by the concentration of ions in the solution. When compounds dissolved in water, they are divided into ions and their ionic strength is expressed by using equation (18) [19].

$$IS_{CaCO3} = \frac{1}{2}[\,[Ca^{+2}] \times (\text{valency of } Ca^{+2} \text{ ion})^2 + [\,[CO_3^{-2}] \times (\text{valency of } CO_3^{-2} \text{ ion})^2] \quad (18)$$

The supersaturation of calcium carbonate ($CaCO_3$) in water is based on two parameters. The saturation index (SI) and PH which can be represented as the PH offset (PH_s) when the actual calcium ion concentration (Ca^{+2}) is in

a balance with the carbonate (CO_3^{-2}).The crystallization driving force is determined by the saturation index (SI). The two indicators are highly attached and utilized for determining the crystallization process performance. The saturation index and the PH offset are determined using equations (19) and (20) respectively.

$$SI = log\frac{[Ca^{+2}] \times [CO_3^{-2}]}{K_s} \quad (19)$$

$$PHs = PH\text{-}SI \quad (20)$$

The change in calcium concentration in equation (21) is determined by the supersaturation of calcium carbonate, the calcite pellets specific surface (S), and the crystallization kinetics (K) [20].

$$\frac{d[Ca^{+2}]}{dt} = K\,.S\,.([Ca^{+2}][CO_3^{-2}] - \frac{k_s}{f^8}) \quad (21)$$

Where, K_s is the solubility product, which is a function to concentrations of calcium and carbonate, and it is calculated by equation (22).

$$Ks = [Ca^{+2}][CO_3^{-2}] \quad (22)$$

Then the modeled calcium concentration as follows:

$$ln[Ca^{+2}]m = -0.175\,.K\,.S\,.[Ca^{+2}]_o[CO_3^{-2}].t + 2.5 \quad (23)$$

Equation (24) is used to calculate the specific surface of calcite pellets (S) as a function of bed porosity (p) and diameter of pellets (d_p).

$$S = \frac{6(1-p)}{dp} \quad (24)$$

The supersaturated water with calcite that transport to seeding material surface relies on the temperature and water flow, the crystallization constant is calculated from equation (25)[21].

$$K = \frac{K_f\,.K_T}{K_f + K_T} \quad (25)$$

The water flow pattern between calcite pellets relies on the Schmidt number (Sc), and the Reynolds number of the water flow in the bed (Re_h). Equation (27) represents the Sherwood number (Sh)[22] .

$$sc = \frac{\nu}{D_f} \quad (26)$$

$$Sh = 0.66Re_h^{0.5}sc^{0.33} \quad (27)$$

Equation (28) is used to determine the coefficient of transportation (K_f).

$$K_f = \frac{Sh\,.D_f}{d_p} \quad (28)$$

The temperature dependency constant (k_T) is calculated by the following equation [22]:

$$K_T = 1.053^{(T-20)}.K_{T20} \quad (29)$$

The crystallization rate:

$$C = \frac{-d[Ca^{+2}]}{dt} = (0.175\,.K\,.S.[Ca^{+2}][CO_3^{-2}]) \quad (30)$$

The mass of crystallized calcium carbonate ($CaCO_3$) can be determined by equation (32) using pellet diameter from equation (15) and the number of sand particles from equation (31).
The number of sand particles is determined using the following equation [23]:

$$N = \frac{As.\Delta x_o.(1-p_0)}{\frac{1}{6}\,\pi\,d_g^3} \quad (31)$$

Therefore, the crystallized mass of calcium carbonate can be found as:

$$mc = N.\left(\tfrac{1}{6}\,\pi\,d_p^3 - \tfrac{1}{6}\,\pi\,d_g^3\right).\rho_c \quad (32)$$

3.3. Modeling work

There are two main models that are commonly used to model pellet softening reactors. The first model is Ergun model (1952)[13] which is the exerted forces on the pellets in the reactor, and the second model is Zaki model (1954) [14]which is based on an expansion formula, because Zaki model is preferred for full scale PR experiment, Ergun model was adopted in this chapter for lab scale PR experiments.

4. Results and Discussions

4.1. Effect of water flow rate on the fluidized bed height and bed porosity

Figures 5, 6, and 7 show that the bed porosity is strongly dependent on the height of the fluidized bed. The porosity was in the range of (0.442 – 0.454) for the bed height of 0.71-0.73 at a flow rate of water of 25 L/hr., (0.2 – 0.6) for the bed height of 0.4-0.9 at water flow rate of 37.5 L/hr., and (0.563-0.565) for the bed height of 0.91-0.93 at water flow rate of 50 L/hr. The value of the water flow rate was 37.5 L/hr. and has many effects on the bed height as a result of interaction took place between the two sand types in comparison with both water flow rates (25, 50 L/hr.) and consequently is reflected in a wide range of porosity variation. For the 25 L/hr. flow rate, the fine particles were dominated bed expansion region while coarse particles were packed together. For the 37.5 L/hr. flow rate, the coarse particles start expanding and mixed with the fine particles, so that a wide range of expanded bed was noticed. And finally for the 50 L/hr. flow rate, the bed expansion was maximized and both particle types (fine and coarse) were fluidized together. However, increasing the water flow rate (Fw) led to increase in the fluidized bed height, then resulted in an increase of bed porosity. This conclusion agrees with the work of Kramer et al. [24], as they demonstrated that increasing of fluidized bed height from (1-4) m increases the bed porosity from 0.72 to 0.85 at water flowrate (Fw= 500 m^3/h), and increasing fluidized bed height from (1-4) m increases the bed porosity from 0.52 to 0.75 at water flowrate (Fw= 300 m^3/h).

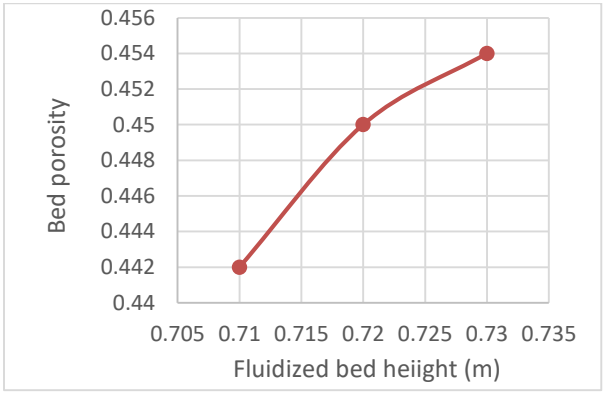

Figure 5: Bed porosity (P) versus fluidized bed height at water flow rate (F_w) = 25 L/h

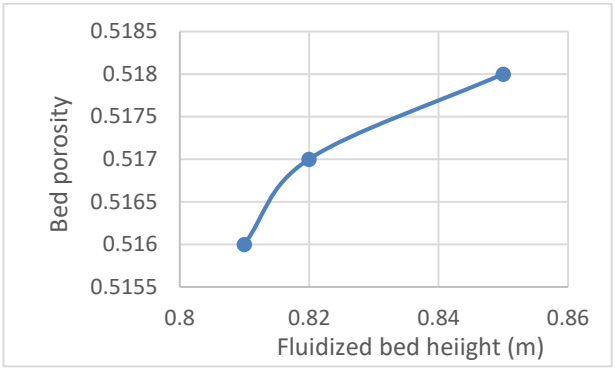

Figure 6: Bed porosity (P) versus fluidized bed height at water flow rate (F_w) = 37.5 L/h

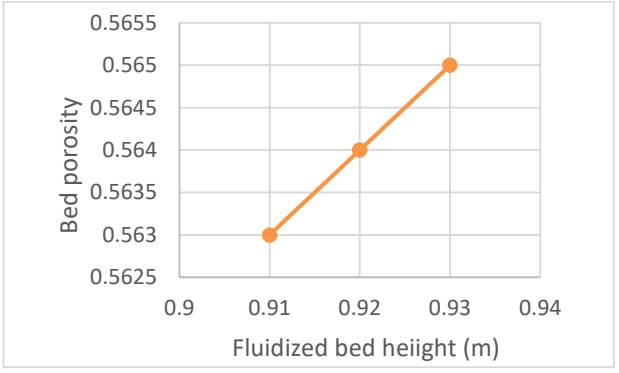

Figure 7: Bed porosity (P) versus fluidized bed height at water flow rate (F_w) = 50 L/h

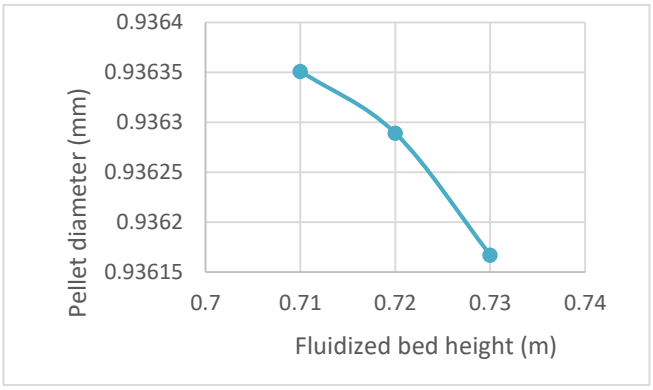

Figure 8: Pellet diameter versus fluidized bed height at water flow rate (Fw) = 25 L/h

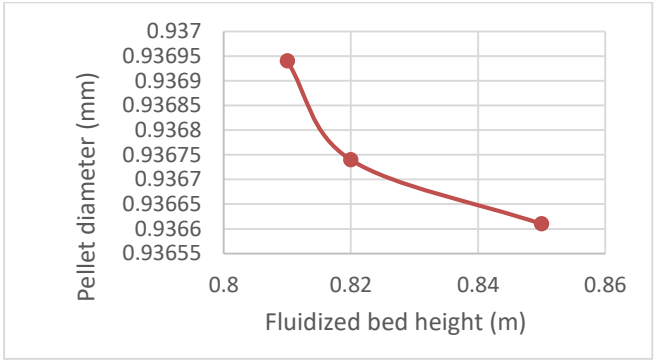

Figure 9: Pellet diameter versus fluidized bed height at water flow rate (F_w) = 37.5 L/h

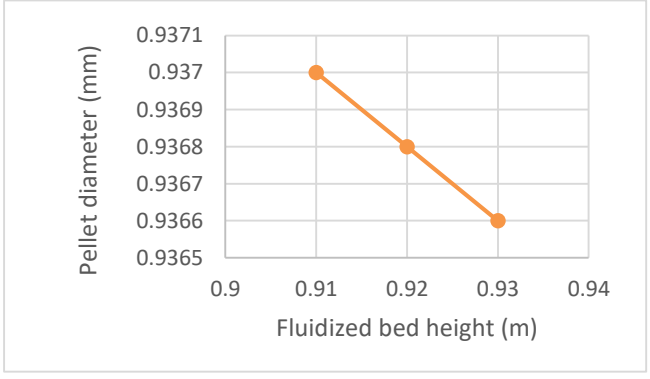

Figure 10: Pellet diameter versus fluidized bed height at water flow rate (F_w)=50 L/h

4.2. Effect of flow rate of water on the fluidized bed height and the pellet diameter and density

Figures 8,9, and 10 show the effect of water flow rate on the expansion of the bed (bed height) and consequently on the pellet diameter. As the bed height increases, the pellet diameter decreases due to higher water upward velocity which causes a higher rate of erosion of the pellet surface. However, for water flow rate of 50 L/hr., the pellet diameter decreased from 0.937 – 0.936 when the bed height increased from 0.81 – 0.85, which is lower than the bed height for flow rates 25, and 37.5 L/hr. This may be due to a probable homogeneity of bed expansion at higher water velocities.

Figures 11, 12, and 13 reflect the effect of bed height on the pellet density for the water flow rates 25, 37.5, 50 L/hr. respectively. The density of pellets decreased as bed height increased. This agrees with **Hu et al**. [25] studies which showed that the highest dense pellets are settled at the bottom of the reactor while the least dense pellets are fluidized at the upper part of the reactor.

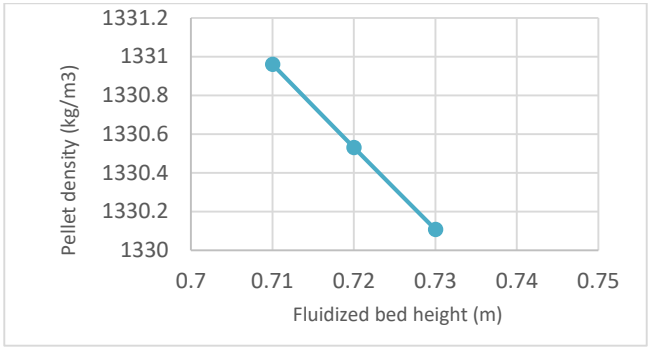

Figure 11: Pellet density versus fluidized bed height at water flow rate (F_w) = 25 L/h

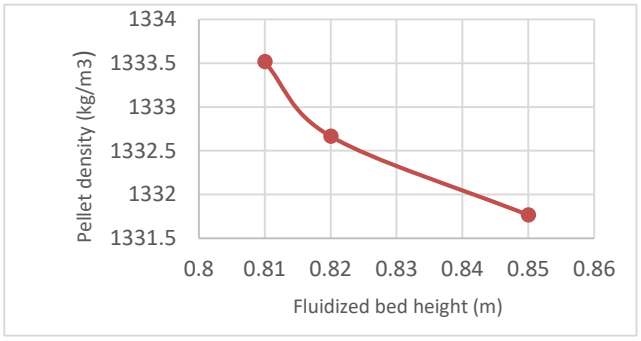

Figure 12: Pellet density versus fluidized bed height at water flow rate (F_w) = 37.5 L/h

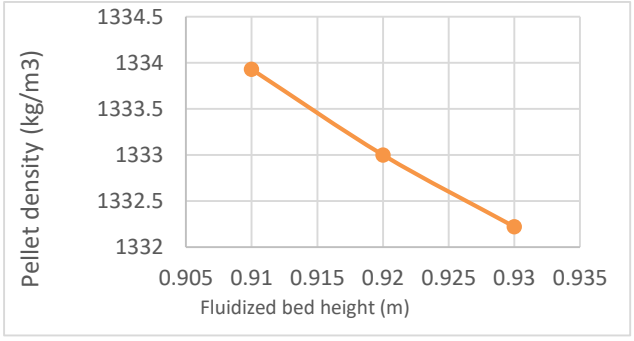

Figure 13: Pellet density versus fluidized bed height at water flow rate (F_w) = 50 L/h

4.3. Comparison between modeled and measured calcium concentrations

Figures 14, 15, and 16 show fair agreement between modeled and measured concentrations of Ca^{+2} ions. The 50 L/hr. water flow rate showed better agreement between modeled and measured concentrations. The higher water flow rates demonstrated good mixing of large and fine particles within the expanded (fluidized) bed and better distribution of Ca^{+2} ions. The 25 L/hr. water flow rate reflects the case where large particles were settled at the bottom of the bed and minor expansion of bed was noticed. This can be attributed to a considerable inhomogeneity of Ca^{+2} ions in the expanded bed. Figure 17 demonstrates that a good agreement between measured and modeled values of calcium ions concentration was noticed for the nine experiments in this research.

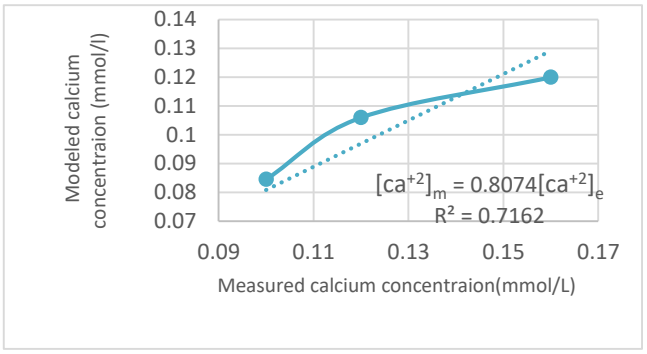

Figure 14: Modeled calcium concentration versus measured calcium concentration at water flow rate (F_w) 25 L/hr.

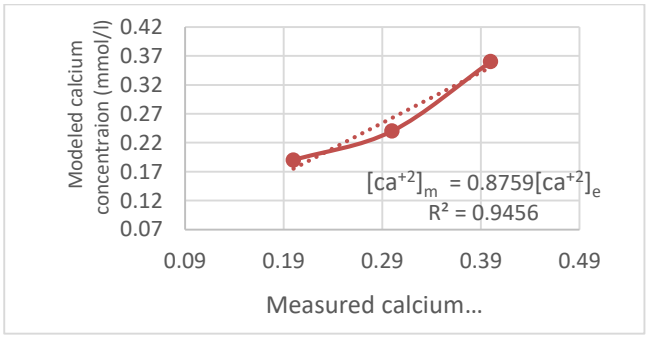

Figure 15: Modeled calcium concentration versus measured calcium concentration at water flow rate (F_w) 37.5 L/h

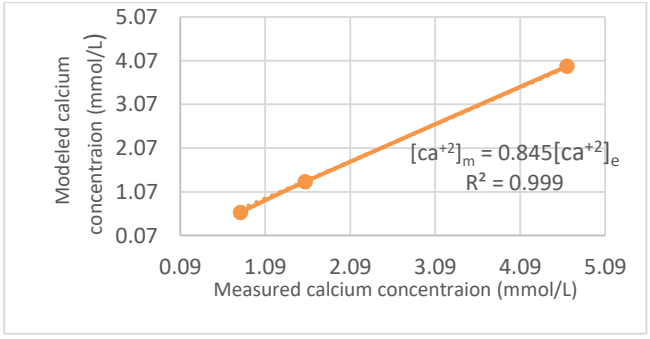

Figure 16: Modeled calcium concentration versus measured calcium concentration at water flow rate (Fw) 50 L/hr.

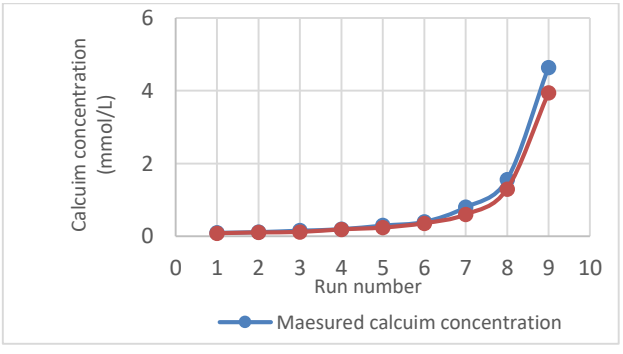

Figure 17: measured and modeled values of calcium ions Concentrations vs. run number

4.4. Comparison between modeled and measured fluidized bed height (m)

A fair agreement between modeled and measured fluidized bed height was observed as shown in Figure 18. However, higher water flow rate results in better agreement between modeled and measured fluidized bed height**.** The correlation coefficient of the fitting in Figure 18 is 0.94, which indicates well correlated data this agreed with **Hu, et al**. [26] which they compared between modeled and measured fluidized bed height, the correlation coefficient of their study was 0.95. Figure 19 shows fair agreement between modeled and measured values of fluidized bed height for the nine experiments in this research work.

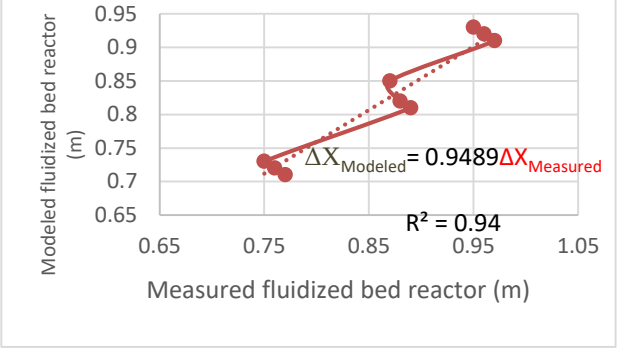

Figure 18: Modeled fluidized bed height versus fluidized bed height at water flow rate (Fw) 25, 37.5, 50 L/hr.

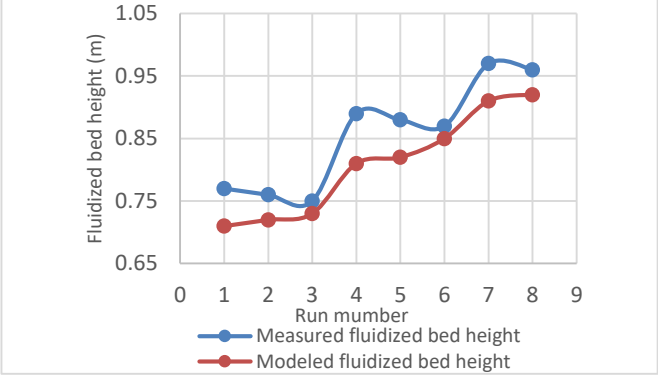

Figure 19: measured and modeled values of fluidized bed Height (m) vs. run number at water flow rate (Fw) 25, 37.5,50 L/hr

4.5. Comparison between modeled and measured calcium carbonates mass (kg) deposited on the surfaces of the pellets

A fair agreement between modeled and measured mass of calcium carbonates deposited on the surfaces of the pellets was observed as shown in Figures 20, 21, and 22. However, higher water flow rate leads to better agreement between modeled and measured mass of calcium carbonates. This also can be attributed to the better homogeneity of fluidized particles of sand in the expanded bed of the pellet reactor. Figure 23 shows fair agreement between modeled and measured values of calcium carbonate mass for the nine experiments in this research work.

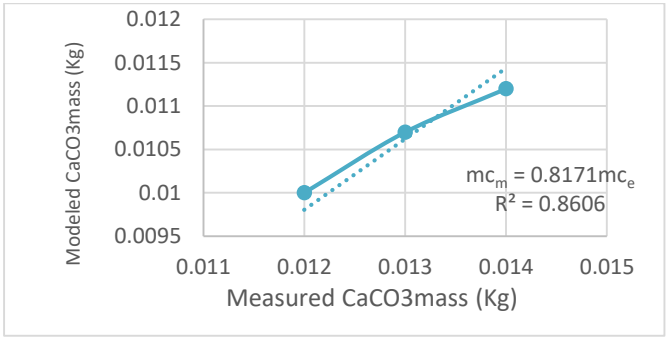

Figure 20: Modeled mass of calcium carbonate versus measured mass of calcium carbonate at water flow rate (Fw) 25 L/hr.

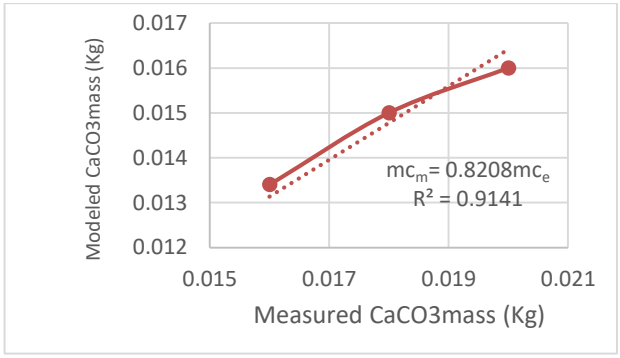

Figure 21: Modeled mass of calcium carbonate versus measured mass of calcium carbonate at water flow rate (Fw) 37.5 L/hr.

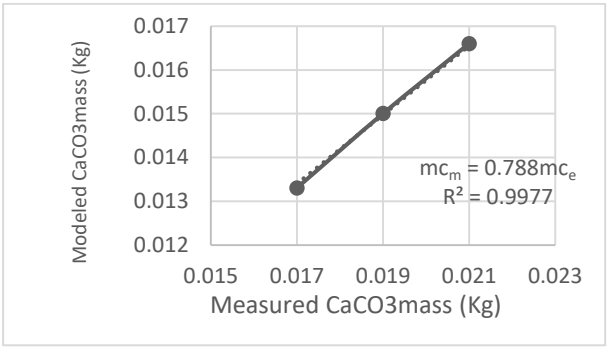

Figure 22: Modeled mass of calcium carbonate versus measured mass of calcium carbonate at water flow rate (Fw) 50 L/hr.

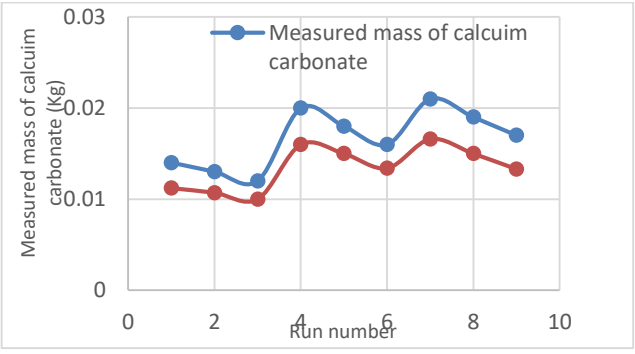

Figure 23: Measured and modeled values of calcium carbonate mass (kg) vs. run number

5. Conclusions

Very high removal efficiencies of total hardness were obtained when flow rates of the groundwater and NaOH solution are properly determined. The obtained results revealed that 78.7 – 99.1% efficiencies can be achieved when the ratio of NaOH solution flow rate to the groundwater flow rate ranges from 0.24 to 0.72 with an initial pH of 7-10.3.

Modeling results of the groundwater softening process using pellet reactor showed that fair agreement between measured and modeled values of the removal efficiency, crystallized mass of calcium carbonates, bed porosity, pellet diameter and density distribution in the expanded (fluidized) bed. The successful modeling of the pellet reactor led to reducing cost of experimentation and may lead to better understanding of groundwater softening processes.

REFERENCES

[1] Hofman, J. A. M. H., Onno Kramer, Jan Peter van der Hoek, Maarten Nederlof, and Martijn Groenendijk, "Twenty years of experience with central softening in Netherlands: Water quality, environmental benefits, and costs," In International Symposium on Health Aspects of Calcium and Magnesium in Drinking Water, pp. 24-26, 2006.

[2] van Houwelingen, G., Bond, R., Seacord, T., & Fessler, E. "Experiences with pellet reactor softening as pretreatment for inland desalination in the USA," Desalination and Water Treatment, 13(1-3), 259-266, 2010.

[3] Tran, A. T., Zhang, Y., Jullok, N., Meesschaert, B., Pinoy, L., & Van der Bruggen, B. , "RO concentrate treatment by a hybrid system consisting of a pellet reactor and electrodialysis," Chemical engineering science, 79, 228-238, 2012.

[4] Palmen, LJ., Schetters, M., van der Hoek, J. P., Kramer, O., Kors, L. J., Hofs, B., & Koppers, H. Production, use and reuse of Dutch calcite in drinking water pellet softening. Poster session presented at IWA world water congress and exhibition, Lisbon, Portugal (2014).
http://resolver.tudelft.nl/uuid:7ff60173-129b-4e5d-a33f-81390a8704bf

[5] Palmen, L. J., Hofs, B., & Koppers, H. , "Circular economy in drinking water treatment: reuse of ground pellets as seeding material in the pellet softening process," Water Science and Technology, 71(4), 479-486,2015.

[6] Mahvi, A. H., Shafiee, F., & Naddafi, K. , "Feasibility study of crystallization process for water softening in a pellet reactor." International Journal of Environmental Science & Technology, 1(4), 301-304,2005.

[7] Chen, Y., Fan, R., An, D., Cheng, Y., & Tan, H. , "Water softening by induced crystallization in fluidized bed," Journal of Environmental Sciences, 50, 109-116.,2016.

[8] Hu, R., Huang, T., Zhi, A., & Tang, Z. , "Full-Scale Experimental Study of Groundwater Softening in a Circulating Pellet Fluidized Reactor," International journal of environmental research and public health, 15(8), 1592,2018.

[9] Van Schagen, K., Rietveld, L., Babuška, R., & Baars, E. ," Control of the fluidised bed in the pellet softening process," Chemical Engineering Science, 63(5), 1390-1400,2008.

[10] Van Schagen, K.l M., Rietveld, L. C., & Babusška, R. , "Dynamic modelling for optimisation of pellet softening," Journal of Water Supply: Research and Technology-AQUA, 57(1), 45-56,2008.

[11] Van Schagen, K. M., Babuška, R., Rietveld, L. C., & Veersma, A. M. J. , "Model-based dosing control of a pellet softening reactor," IFAC Proceedings Volumes, 42(11), 267-272,2009.

[12] Hu, R. Z., Huang, T. L., Wen, G., & Yang, S. Y. , "Modelling particle growth of calcium carbonate in a pilot-scale pellet fluidized bed reactor," Water Science and Technology: Water Supply, 17(3), 643-651,2017.

[13] Ergun, S., "Fluid flow through packed columns. Chem.Eng.Progr," 48(2), 89–94. 1952.

[14] Van Dijk, J.C. and D.A. Wilms, Water treatment without waste material - fundamentals and state of the art of pellet softening," Journal of Water Supply: Research and Technology-AQUA Vol 40(5), 263–280, 1991.

[15] Rietveld, L.C. ," Improving operation of drinkingwater treatment through modeling," Ph. D. thesis, Faculty of Civil Engineering and Geosciences, Delft University of Technology,2005.

[16] Tai, Clifford Y. and Hsiao-Ping Hsu," Crystal growth kinetics of calcite and its comparison with readily soluble salts," Powder Technology 121, 60–67, 2001.

[17] Van Schagen, K. M., "Model-based control of drinking-water treatment plants, 2009.

[18] Van Dijk, J.C., Wilms, D.A. , "Water treatment without waste material-fundamentals and state of the art of pellet softening," Journal Water SRT-Aqua, Vol. 40(No. 5), 263-280,1991.

[19] Graveland, A., Dijk J.C. van, Moel, P.J. de, Oomen, J.H.C.M. ,"Developments in water softening by means of pellet reactors," Journal AWWA, 619-625,1983.

[20] Wiechers, H.N.S., P. Sturrock and G.v.R. Marais, "Calcium carbonate crystallization kinetics," Water Research 9, 835–845, 1975.

[21] Karpinski, P.H. , "Crystallization as a mass transfer phenomenon," Chemical Engineering Science 35, 2321–2324, 1980.

[22] Budz, J., P.H. Karpanski and Z. Nuruc," Influence of hydronamics on crystal growth and dissolution in a fluidized bed," AIChE Journal 30(5), 710–717,1984.

[23] Schetters, M. J. A., " Grinded Dutch calcite as seeding material in the pellet softening process," 2013.

[24] Kramer, O. J. I., Jobse, M. A., Baars, E. T., van der Helm, A. W. C., Colin, M. G., Kors, L. J., & van Vugt, W. H. , "Model-based prediction of fluid bed state in full-scale drinking water pellet softening reactors,". In The Royal Dutch Water Association and the International Water Association. IWC International Water Conferences, 2015.

[25] Hu, R., Huang, T., Zhi, A., & Tang, Z.,"Full-Scale Experimental Study of Groundwater Softening in a Circulating Pellet Fluidized Reactor," International journal of environmental research and public health, 15(8), 1592, 2018.

[26] Hu, R. Z., Huang, T. L., Wen, G., & Yang, S. Y. ,"Modelling particle growth of calcium carbonate in a pilot-scale pellet fluidized bed reactor," Water Science and Technology: Water Supply, 17(3), 643- 651,2017.